EUROPEAN ORGANIZATION FOR NUCLEAR RESEARCH

CERN-EP/2002-099
16 December 2002

VUV Absorbing Vapours in n-Perfluorocarbons.

E. Albrecht[2], G. Baum[1], T. Bellunato[2], A. Bressan[3], S. Dalla Torre[3], C. D'Ambrosio[2], M. Davenport[2], M. Dragicevic[2], S. Duarte Pinto[2], P. Fauland[1], S. Ilie[2], G. Lenzen[4], P. Pagano[3], D. Piedigrossi[2], F. Tessarotto[3] and O. Ullaland[2]

[1] University of Bielefeld, Bielefeld, Germany

[2] CERN, Geneva, Switzerland

[3] INFN Trieste and University of Trieste, Trieste, Italy

[4] Gesamthochschule Wuppertal, Bergische Universitaet, Wuppertal, Germany

Abstract

The optical transparency of perfluorocarbons used as Cherenkov media is of prime importance to many Ring Imaging Cherenkov detectors. We will in this paper show that the main photon absorbers in these fluids are hydrocarbons with double or triple bonds. We will moreover discuss a process which can eliminate these pollutants and restore the intrinsic excellent optical transparency of these fluids in the VUV range.

1 Introduction

Perfluorocarbon gases are widely used as Cherenkov media as they span a wide range of refractive indices, they are chemically inert and they have the cut-off wavelength below 80 nm for room temperature gases. The pure gases are also fully transparent well below 160 nm. This, together with the reasonable small chromatic aberration, makes them particularly valuable as Cherenkov radiators in detector systems which use VUV sensitive photon converters like TMAE (Tetrakis(dimethylamino)ethylene $C_{10}H_{24}N_4$) [1], TEA (Triethyl amine $C_6H_{15}N$) [2] and CsI [3]. Some properties of the first n-fluorocarbons are given in table 1.

Fluorocarbon		Boiling point °C	Sellmeier A $\times 10^{-6}$	Sellmeier λ_0 nm	Reference
CF_4	Tetrafluoromethane	-128.06	0.1164	61.81	[4]
C_2F_6	Perfluoroethane	-78.2	0.1746	66.75	[5]
C_3F_8	Perfluoropropane	-36.7	0.2305	67.90	[6]
C_4F_{10}	Perfluoro-n-butane	-1.9	0.2375	73.63	[7]
C_5F_{12}	n-Perfluoropentane	29.2	0.1986	86.57	[7]
C_6F_{14}	Perfluoro-n-Hexane	56	56.8	66.54	[8]

Table 1: Some properties of fluorocarbons. A and λ_0 refer to the Sellmeier parameterisation of the refractive index as $(n-1) = A/\left[\lambda_0^{-2} - \lambda^{-2}\right]$. A is given for the gas at NTP.

Perfluorocarbons, as fluorocarbons, are equivalent to hydrocarbons where the hydrogen atoms are replaced by fluorine atoms. Alkyl halides are classified as primary, secondary, or

tertiary according to the degree of substitution at the carbon to which the halogen is attached. In a primary alkyl halide, the carbon that bears the halogen is directly bonded to one other carbon, in a secondary alkyl halide to two, and in a tertiary alkyl halide to three.

Different preparation methods are used to obtain fluorine containing organic substances. We will list some of them here:

- Direct fluorination of hydrocarbons in the presence of Cu or Ag.
- Indirect fluorination using metal fluorides like CoF_3, CeF_4 or MnF_3, as fluorinating agents.
- Halogen exchange reaction like $C_2H_5Br \xrightarrow{F_2Hg} C_2H_5F$
- Addition of multiple bonds as in the reaction
  $HC{\equiv}CH{+}HF \longrightarrow H_2C{=}CHF{+}HF \longrightarrow H_3C{-}CHF_2$
- Pyrolitic reactions as in $2CHF_2Cl \xrightarrow{700\,^\circ C} F_2C{=}CF_2{+}2HCl$
- Electrolytic methods are also used.

The reactions involving F_2 molecules are strongly violent and exothermic, as compared to Cl_2. For instance:

$R3C{-}H + X_2 \rightarrow R3C{-}X + HX$	$\Delta H(X{=}F) = -\,103\,\text{kcal}$	$\Delta H(X{=}Cl) = -\,23\,\text{kcal}$
$R2C{=}CR2 + X_2 \rightarrow R2CX{-}XCR2$	$\Delta H(X{=}F) = -\,107\,\text{kcal}$	$\Delta H(X{=}Cl) = -\,33\,\text{kcal}$

These reactions are controlled by the dilution of reactants using inert gases or in presence of copper or silver sieves. In this case the probable fluorinating agent is AgF_2 which appears in the reaction medium [9].

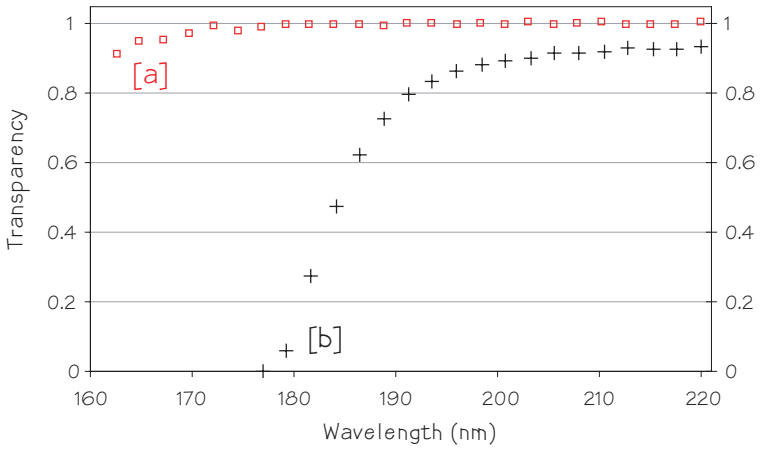

Figure 1: Transparency of two samples, [a] and [b], of C_4F_{10} for a 15 cm long absorption length at NTP.

Even though the pure perfluorocarbon molecule is fully transparent in the far UV range, the raw gas as received is not always usable as a Cherenkov radiator medium. An example of this is shown in figure 1. It has also proven very costly both in resources and in material, to obtain and to maintain the required transparency of the fluid [10]. It has therefore become imperative to search for the possible contaminants and to establish a method to eliminate them. If at all possible, this process ought to be easy, straightforward and should require low overhead.

We will in this paper discuss different admixtures which will strongly enhance the photon absorption in these fluids together with their specific absorption signatures in the VUV range. We will in section 5 review the most common and efficient methods to isolate and eliminate these

impurities. Section 6 is devoted to the work of establishing a correlation between these known absorption bands and the absorption signatures measured in perfluorocarbon gas. Once this connection has been well established, we will demonstrate an efficient method to isolate these molecules from the perfluorocarbons and thereby fully restoring the transparency of the fluid. Section 2 gives an overview of the instruments which have been used to qualify the transparency of the fluorocarbons in the VUV range.

2 Experimental procedure

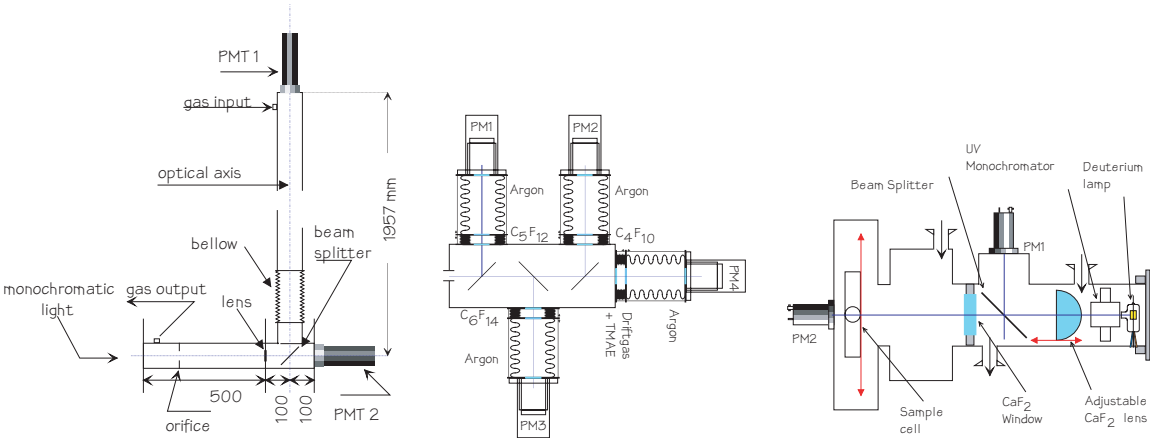

Figure 2: Sketches of the working principle of the measuring systems.

Our most recent data on gas transparency is taken with the set-up sketched in figure 2 (a). A ~ 2 m long light absorption chamber is built around a deuterium lamp with a Seya-Namioka monochromator [11]. Two photo multipliers [1] with wavelength shifters [2] are used for light detection. The monochromatic light beam enters the gas tube where it is focused by a lens onto photo multiplier #1. The light beam is split by the beam splitter between the lower, the reference, photo multiplier #2 and the upper one. The difference in light path length between the two photo multipliers is 185.7 cm. The windows, as well as the lens and the beam splitter, are made of calcium fluoride. The system can thereby measure in the wavelength range from ~ 154 to 500 nm. The spread is estimated to be 0.7 nm and the overall absolute calibration error to ± 0.25 nm. The anode currents from the photo multipliers are read via pA meters [13]. Reference spectra are taken with argon. The data acquisition and the running of the data taking is fully automatic [3].

A similar system was used previously and it is sketched in figure 2 (b). It used the same monochromator system, but used variably length cells for the measurement of the transparency of the fluids [11]. The windows and the beam splitters were made from fused silica quartz which limited the lower wavelength to ~ 163 nm. The maximum light attenuation length was 15 cm.

A third system is sketched in figure 2 (c). It is based on the CERN reflectometer [12], which has been modified to allow for light transmission measurement down to 155 nm. The UV-monochromator selects the wavelength of the light emitted by the deuterium lamp. Each single measurement is performed in the wavelength region between 160 and 230 nm. Uniform focusing

[1] Thorn EMI, type 9884 B
[2] 1 μm paraterphenyl and 25 nm MgF_2
[3] LabView system by National Instruments

of the beam is achieved with a position adjustable calcium fluoride lens. A beam splitter allows for normalisation measurements, by directing part of the beam to photo multiplier PM1. The lamp, the monochromator and the light path to PM1 are housed in the monochromator chamber which is kept transparent by a constant argon flow. The measuring cell, 5.1 cm long, closed along the light path by two calcium fluoride windows, is mounted on a gear rod in the vacuum chamber. It is separated from the monochromator chamber by a calcium fluoride window. The photo multiplier PM2 is measuring the intensity of light downstream of the measuring cell. As the cell is movable, three different measurements are possible. The background is quantified by absorbing the light beam on a black coated metallic plate, the reference measurement is performed filling the cell with nitrogen and the actual measurement when the cell is filled with liquid C_4F_{10}. The measured values are corrected for the light transmission losses at the surface between media of different refractive index.

3 Atmospheric gases as UV photon absorbers

We will in this and in the following section give a brief description of common molecules that will absorb photons in the wavelength range below 200 nm. We will give a short discussion of the main absorption bands and furthermore express the effect of the pollutants on the transparency by simple mathematical models.

Atmospheric gases are the most common photon absorbers in the wavelength range below 200 nm. This is primarily due to leaks or diffusion between the Cherenkov radiator structure and the surrounding air. It is also due to the fairly high solubility of certain vapours in perfluorocarbons. An example is given in table 2.

Water	ppm	11
Oxygen	ml gas/100 ml	65
Carbon dioxide	ml gas/100 ml	248
Helium	ml gas/100 ml	11
Argon	ml gas/100 ml	65
Nitrogen	ml gas/100 ml	43
Ethane	ml gas/100 ml	282

Table 2: Solubility of some common substances in liquid C_6F_{14} [14].

The absorption coefficient for water, figure 3, is fairly well described down to 125 nm by a superposition of three gaussian distributions. The mean and the sigma of these curves are given as (128.0,5.75), (162.7,7.28) and (172.9,4.49) in units of nm. The absorption here is almost entirely due to the continuum with a maximum at about 165.5 nm. There is moreover some indication of some very weak bands. Below 140 nm, a number of diffuse bands are found superimposed on the second continuum. The interval between these bands is about 800 cm^{-1}. Photon absorption by water does therefore not play any significant role in a practical Cherenkov detector above $\sim$ 186 nm. Further discussion can be found in reference [15].

The absorption coefficient for oxygen through the Schumann-Runge band down to 140 nm is similarly described by one gaussian distribution where the mean and the sigma is given as (142.9,11.6) in units of nm. The photon absorption cross section of the underlying continuum of the Schumann-Runge band in the wavelength range from 175 to 242 nm is dominated by the photo dissociation of O_2. The upper limit is given by dissociation limit of the $O(^3P)$+$O(^3P)$ ground state, $X^3\Sigma_g^-$, and the lower limit by the dissociation of the lower state of $O(^3P)$+$O(^1D)$, $B^3\Sigma_u^-$. The continuum gradually increases towards smaller wavelength and almost levels off at around 198 nm. It then increases rapidly to a value of 7.1×10^{-22} cm^2 at 181.4 nm. This is still

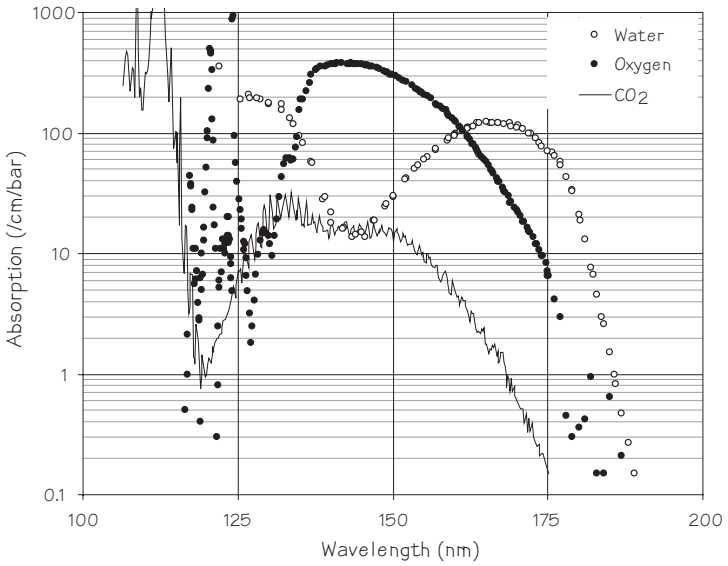

Figure 3: Photon absorption coefficient [15] for oxygen, water and carbon dioxide as function of wavelength.

a small number and the photon absorption in O_2 above 180 nm can therefore be neglected for all practical gas Cherenkov detectors. Further discussion of photon absorption in O_2 can be found in [15], [16] and [17] and references therein. The absorption coefficient is plotted in figure 3. As can be seen from the discussion in [15], O_3 has a strong continuum with a maximum at 255 nm. O_3 is however not a likely pollutant for Cherenkov radiators.

CO_2 has a photon absorption coefficient which can be well described down to 220 nm by a sum of two gaussian. The mean and the sigma of these two distributions are given in nm by (131.9,4.75) and (145.8,9.43). The absorption coefficient is plotted in figure 3. The bands overlaying the continuum above 140 nm are mainly irregular and diffuse. Below 140 nm they appear to be more regular and intense. The absorption continuum arises probably from the relatively steep repulsive curve for the dissociation products $CO(^1\Sigma)+O(^3P)$. The overall photon absorption coefficient down to 120 nm is generally not very strong and can be considered as insignificant above 170 nm. More information can be found in references [15] and [16].

4 Hydrocarbons as UV photon absorbers

Measurements of the ultraviolet absorption spectra of hydrocarbons have been done since the early days of spectroscopy. These bands presented the first conclusive examples of an electronic transition forbidden by the symmetry selection rules and an application of the vibronic selection rules. The interest of photon absorption and dissociation of hydrocarbons have increased again during the last years as a result of the search for organic polymer formation and thereby haze particles, in planetary atmospheres.

Hydrocarbons are classified depending on the bonds between the carbon atoms. Alkanes, alkenes, alkynes and aromatics have respectively single bonds, a double bond, a triple bond or three pairs of conjugated double bonds between the atoms. The photon absorption coefficient for some alkanes are plotted in figure 4 (a).

It can be seen from figure 4 (a) that methane, ethane, propane and n-butane have all very similar photon absorption curves and that the turn-on of the absorption can be approximated to $\lambda_{\mathrm{turn-on}} = 181 - \frac{226}{2+N}$ where N is the number of bonds and λ is in nm. It can furthermore

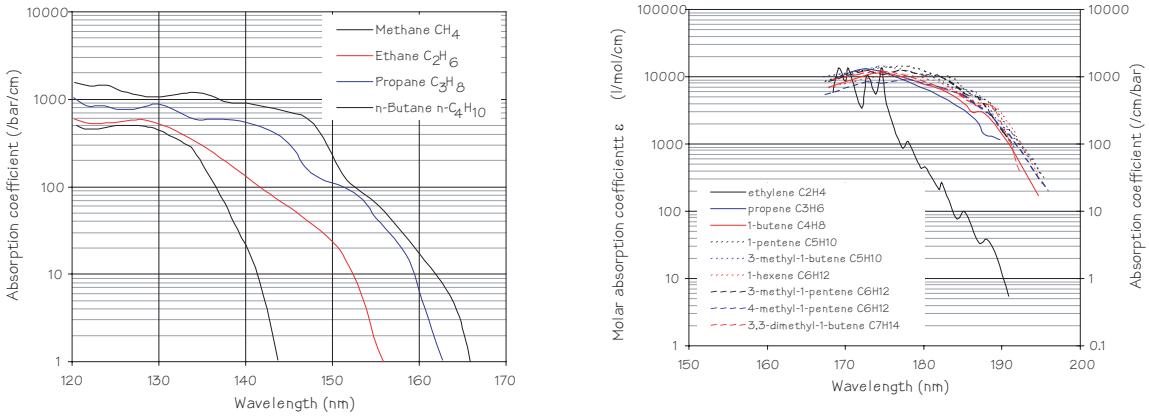

(a) (b)

Figure 4: Photon absorption coefficient for (a) alkanes and (b) for alkenes. (a) is for atmospheric pressure and 25 °C. The decatic molar absorption coefficient, ε, is defined by A=-$\log_{10}$T=$\varepsilon\times$b$\times$c, where b is the path length in cm and c is the molar concentration in mol/litre. The right-hand axis of (b) gives the absorption coefficient in units of /cm/bar for c=0.044 mol/l. Data replotted from reference [18] and [19].

be observed that as the number of bonds increases, wide bands will overlay the absorption continuum.

This picture changes dramatically when going to molecules with double bonds. The decatic molar absorption coefficient [4], ε, for some hydrocarbons with a single double bond is plotted in figure 4 (b). ε is defined by A=-$\log_{10}$T=$\varepsilon\times$b$\times$c, where b is the path length in cm and c is the molar concentration in mol/litre. We observe that ε for all these alkenes, apart from ethylene, can be approximated down passed 170 nm with a single gaussian with a mean and a sigma given as (175,7) in units of nm. The $\lambda_{\text{turn-on}}$ is in the range of 210 nm. Ethylene is different. We observe here very strong and periodic bands overlying the continuum. $\lambda_{\text{turn-on}}$ for ethylene is in the range of 200 nm.

The picture is further confused when going from simple olefins to diolefins, hydrocarbon molecules with two double bonds between the carbon atoms. The maximum of the absorption band shifts regularly towards the visible with increased number of conjugated double bonds. The molar absorption coefficient is very high with $\varepsilon \sim 10^4$ l/mol/cm. This corresponds to the promotion of an electron from the π system to an antibonding π^* orbital. It is of course not excluded that these more complex structures are responsible for the loss of transparency in perfluorocarbons in the VUV range. It is however futile to search for them without a clear signature in the absorption spectra.

The simplest molecule in the acetylenic series, or alkynes, is acetylene, C_2H_2, and the first of the aromatic hydrocarbons is benzene, C_6H_6. Benzene shows a broad absorption band in the near UV with a maximum at around 256 nm. This is in principle a forbidden transition, $^1B_{2u} \leftarrow {}^1A_{1g}$. It is weak as it is allowed via the interactions with molecular skeleton vibrations. The second forbidden band in benzene is at about 200 nm for the transition $^1B_{1u} \leftarrow {}^1A_{1g}$. The intense allowed transition, $^1E_{2u} \leftarrow {}^1A_{1g}$, is at about 180 nm. The absorption spectrum is plotted in figure 5 (a). Our measurement is well described by previously published data in [20], [21] and [22] apart from in the small wavelength range between 163 to 175 nm. We will use our measurement throughout this paper.

[4] Formerly molar extinction coefficient

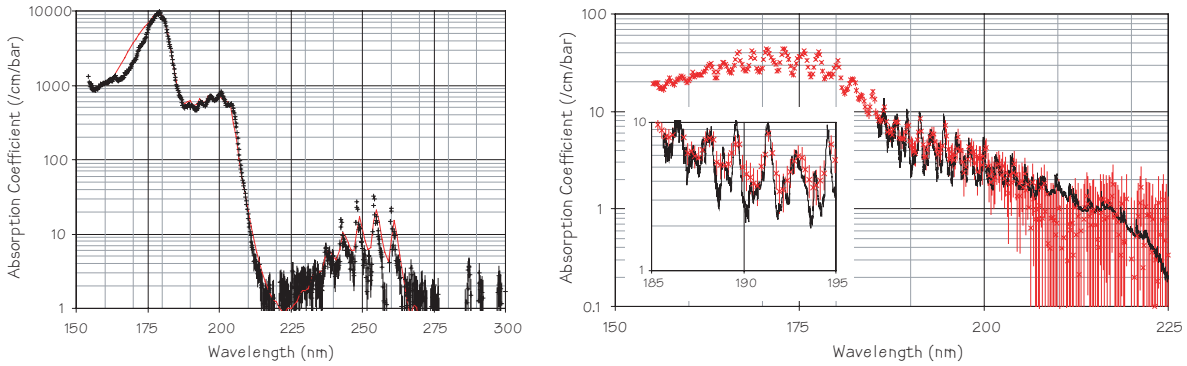

(a) (b)

Figure 5: (a) is the photon absorption coefficient for C_6H_6. + is our measurement and the solid line is data replotted from reference [20], [21] and [22]. (b) is the photon absorption coefficient for C_2H_2. × is our measurement. The line is data from [23].

Acetylene has a broad absorption spectrum, figure 5 (b), with a maximum at around 170 nm. Overlying this continuum are distinct bands. This absorption system is dominated by a long progression in the trans-bending mode and a combination of C−C stretching. For each of the stronger bands, a progression in the lower state trans-bending mode can be observed in the high resolution data from [23] together with sub-bands. It can furthermore be shown that the singlet state is perturbed by Fermi interactions and that some couplings exist with an isoenergetic triplet state. All this leads to the fairly complicated absorption spectra in figure 5 (b). Our measurement is in perfect agreement with data given in [23] apart from the loss of statistical significance in our data above 200 nm. We will use our data below 188 nm and the data from [23] above this wavelength.

5 Adsorbers

Adsorbents are the most commonly used material to clean gases or liquids. More recently thin film capillary membranes [25] have been used for separation and isolation. This work is mainly governed by the interest to separate H_2 from CH_4, CO and N_2 gases.

Adsorption is the process of retaining the molecules on the surface of a solid body. Synthetic zeolits or metal alumino silicates [24] have a network of pores which are strictly defined as 3, 4, 5 or 10 Å. Other adsorbents like silica gel and activated alumina, have a wide pore distribution. In activated carbon particle, pores of different sizes are found. Pores can be distinguished into micropores with a radius below 2 nm, mesopores with radius in the range of 2-50 nm and macropores where the radius is larger than 50 nm. Micro- and mesopores give the carbon its adsorptive capacity. They are formed during the process of activation. Granular activated carbons have also macropores. These allow a rapid access to the meso- and micropores, where the actual adsorption takes place.

The choice of an adsorbent is defined by the kinetic diameter [5] of the molecule to be retained

[5]The kinetic or collision diameter is the intermolecular distance of closest approach for two molecules colliding with zero initial kinetic energy. For spherical and nonpolar molecules the potential energy of interaction, $\phi(r)$, is well described by the Lennard-Jones potential $\phi(r) = 4\epsilon\left[(\frac{\sigma}{r})^{12} - (\frac{\sigma}{r})^{6}\right]$. σ and ϵ are constants which are characteristic to the molecule and are determined from second virial coefficients. In assessing the apparent pore size of molecular sieve zeolites, the critical dimensions for spherical molecules are given when $\phi(r) = \epsilon$, or $r_{\min} = \sqrt[6]{2}\sigma$. For diatomic molecules, $r_{\min}$ is based upon the van der Waals length and represents the molecule in all orientations. For long molecules, like hydrocarbons, the diameter is the minimum cross-sectional diameter.

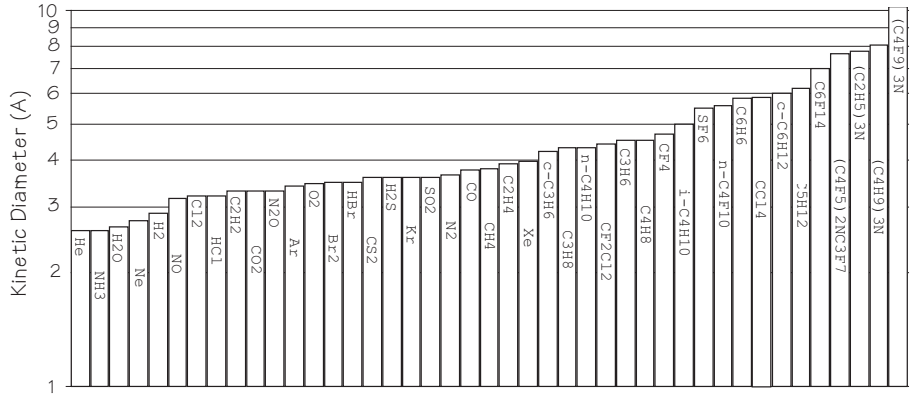

Figure 6: Kinetic diameter for some molecules [24].

together with characteristics like the dipole moment and the polarizability of the molecule. The adsorption rate is also a function of the temperature and the pressure. Figure 6 gives the kinetic diameter of some common molecules. Water is easily adsorbed in molecular sieves of 3 or 4 Å to a level well below a ppm. Oxygen is most commonly removed by either a flushing of the fluid by an inert gas like N_2 or Ar, or by using a catalyst like Cu or Cr. Highly dispersed copper on a zeolite support will have a high specific surface of some $10^2 - 10^3$ m^2/g. This is a good catalyst which is commonly used in industry. It is also an efficient oxygen remover at room temperature through the reaction $4\,Cu + O_2 \rightarrow 2\,Cu_2O$. In this case the copper acts as an ordinary reactant towards the oxygen. The reaction is exothermic and therefore overheated local zones might be formed. If potentially reactive or non-inert nucleon species are present, this oxygen remover will act as a catalyst [26] as in the reaction

$$\mathrm{R-\overset{\overset{H}{|}}{\underset{\underset{F}{|}}{C}}-\overset{\overset{F}{|}}{\underset{\underset{F}{|}}{C}}-F \xrightarrow[Cu/zeolite]{-HF,\ t^\circ} R-\underset{\underset{F}{|}}{C}=\overset{\overset{F}{|}}{C}-F}$$

The presence of these double bonds, even in small concentration, will strongly decrease the optical transmission of the fluorocarbon matrix as a consequence of their high molar absorption coefficient.

Molecular sieves are mainly used for a targeted adsorption whereas activated carbon has proven particularly effective to remove aromatics as well as aliphatics from a fluid.

6 Discussion

From the discussion in section 3 together with figure 1, it is clear that the main pollutants from air will not alone describe the loss of transparency above 180 nm. Likewise it has been shown that it is possible to remove the main photon absorption components from the perfluorocarbon fluids by massively cleaning it with molecular sieves together with activated carbon or by catalysts.

Table 3 shows the relative concentration of detected molecules in a VUV transparent, good, and a non-transparent, bad, fluid. The data is taken with a NMR probe. It is difficult to draw any conclusion from the apparent differences between the composition of a good and a bad perfluorocarbon fluid as shown in table 3, as the VUV transmission properties for some of these molecules are badly known. There are clearly present not fully fluorinated molecules of the type n-$C_4F_{10-i}H_i$ on a level of 0.26 %. These molecules are normally fully transparent in the VUV. The role of sulphur in some of these molecules is unknown.

Component Structure †	NMR Relative Wt. % Concentration $CF_3CF_2CF_2CF_3$ Good	$CF_3CF_2CF_2CF_3$ Bad
$CF_3CF_2CF_2CF_3$	93.6	93.4
$(CF_3)_3CF$	5.46	5.87
$CF_3CF_2CF_2CF_2CF_2CF_3$	0.28	not detected
$(CF_3)_2CFCF_2CF_2CF_3$	0.080	not detected
$(CF_3)_3$-N	0.054	0.080
CF_3-CF_2-O-CF_2-CF_3	0.036	0.036
$CF_3CF_2CF(CF_3)CF_2CF_3$	0.024	not detected
$(CF_3)_2CFCF(CF_3)_2$	0.011	not detected
$(CF_3)_3CCF_2CF_3$	0.0080	not detected
$CF_3CF_2CF\mathbf{H}CF_3$	not detected	0.14
$CF_3CF_2C\mathbf{H}_2CF_3$	not detected	0.092
$(CF_3)_2$-N-$CF_2\mathbf{H}$	not detected	0.036
$CF_3CF_2CF_2CF_2\mathbf{H}$	not detected	0.025
$FC\mathbf{H}_2SF_4F$	not detected	0.0076
$\mathbf{H}_3CSF_4F$	not detected	0.0065
F_3CSF_4F	not detected	0.0037
c-C_4F_8	not detected	0.0030
$C\mathbf{H}_3CF_2CF_2CF_3$	not detected	0.0022

Table 3: Overall $^1H/^{19}F$-NMR Cross Integration Quantitative Compositional Results. † Trace amounts of other unassigned protonated and fluorinated components are also detected in the spectra. Data from [27].

Figure 7 (a) shows the mass spectra for a raw C_4F_{10} gas. Figure 7 (b) shows the relative abundance of elements between the raw and a clean gas. The clean gas was transparent in the VUV whereas the raw gas had much the same behaviour as sample [b] which is shown in figure 1. The sensitivity of the measurement is estimated to be about 10^{-4}. All the major lines in C_4F_{10} are well described with a possible admixture of C_iF_{2i+2} on about a percent level. The combination of the lines 28, 29 and 32 are attributed to C_iH_{2i+2} with a possible trace contamination of CFH and C_iH_j. There are clear lines appearing in the raw gas that are not reproduced in the clean one. These are lines like 51, 72, 82, 96, 113, 114 up to 203. We have been unable to attribute these lines to any likely molecule or combinations of probable molecules.

Further investigations have been done by IR spectrometer analysis [26]. These measurements established the presence of C−H bonds within the raw fluorocarbon fluid. It should be noted that only the impurities which showed a specific IR absorption around 3000 cm^{-1} would give rise to an optical transmission loss after being processed with dispersed Cu or Cr. Pure hydrocarbons are not affected by contact with these oxygen absorbers. It was furthermore shown that the loss of transparency was due to the not fully fluorinated fluorocarbons.

Based on the observation of not fully fluorinated molecules, we have investigated the possibility that the loss of transparency is due to trace amounts of hydrocarbons dissolved in the fluid. Figure 8 (a) shows a measurement of a partially cleaned C_4F_{10} gas together with a possible fit to the data. The gas had been cleaned by a catalyst [6].

The general trend of the data is well described down to 165 nm by an admixture of C_2H_2 at 130 ppm, C_2H_4 at 11 ppm, other alkenes at 0.3 ppm and C_6H_6 at 0.3 ppm. The uncertainty on these parameters is about 10 %. Water and oxygen content in the sample is set to 0 ppm. The

[6] Oxisorb, Messer Griesheim AG. http://www.spezialgase.de

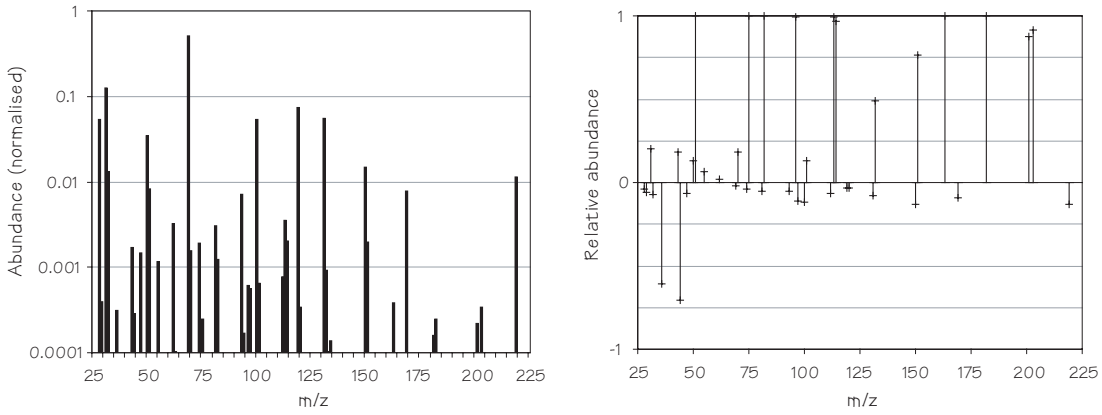

(a) (b)

Figure 7: (a) Abundance of elements as function on m/z for a raw C_4F_{10} gas. The integral is set equal 1. (b) is the relative abundance of elements as function on m/z for a raw and a clean C_4F_{10} gas defined by the ratio $[\text{Abundance}_{\text{raw}} - \text{Abundance}_{\text{clean}}]/[\text{Abundance}_{\text{raw}} + \text{Abundance}_{\text{clean}}]$.

molar concentration for all the hydrocarbons has been set to $c_{C_6H_6}$=0.044 mol/litre. There has been no attempt to fit the data below 165 nm as our knowledge of the absorption spectra for the alkenes below this wavelength is very limited.

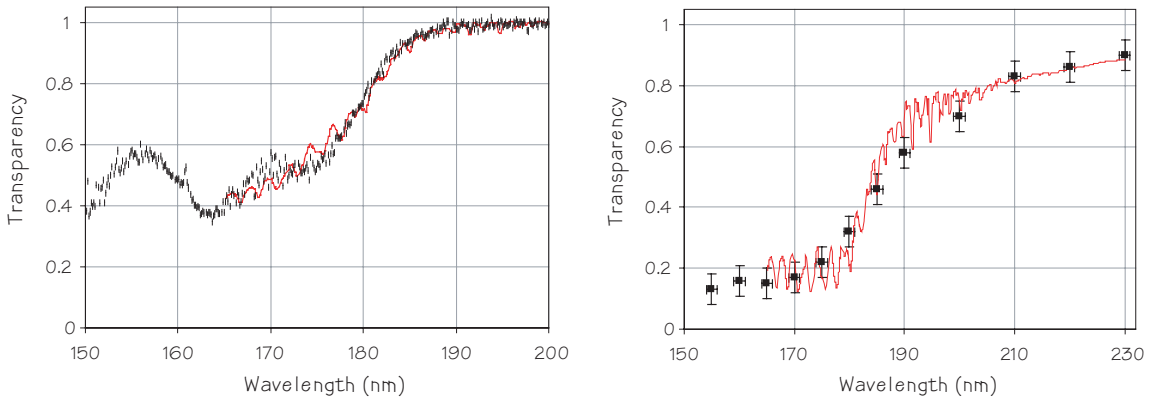

(a) (b)

Figure 8: (a) Transparency of a sample of C_4F_{10} for a 20 cm long absorption length at 2.3 bar absolute. The solid line is a possible fit with C_2H_2 at 130 ppm, C_2H_4 at 11 ppm, other alkenes at 0.3 ppm and C_6H_6 at 0.3 ppm. (b) Transparency of a sample of C_4F_{10} for a 500 cm long absorption length at NTP. The solid line is a possible fit with C_2H_2 at 75 ppm, C_2H_4 at .025 ppm, other alkenes at 0 ppm and C_6H_6 at 0.05 ppm. Oxygen and water is set to the measured value of 2 ppm. Rayleigh scattering is also added for the 5 meter scattering length.

The absorption spectrum for benzene was shown in figure 5 (a). The finding of a possible admixture of benzene to the gas is very promising as this molecule has a number of well defined absorption lines in the wavelength range from 240 to 270 nm. There is a progression of absorption lines with a spacing of 160 cm^{-1} which can be interpreted as $n - n$ transition of the E_u^+C vibration [21]. To investigate this possibility, raw C_4F_{10} gas was passed through activated carbon until the carbon was fully saturated. The carbon filter was then heated to 90 °C and argon was flowed through it. The resulting gas was then analysed by a monochromator. The

result is plotted in figure 9 (a). A reasonable good fit to the data is obtained with a sinusoidal with a period of 160 ± 5 cm^{-1}. It should be noted that the resolution of the monochromator is about 0.7 nm. The uncertainty on the absolute wavelength calibration is about ± 0.25 nm. Figure 9 (b) shows the fluorescence of benzene in this wavelength range.

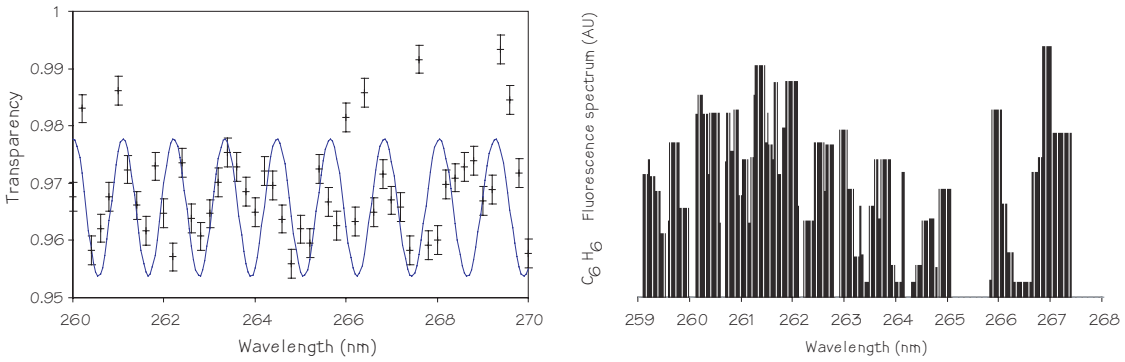

(a) (b)

Figure 9: (a) is the photon absorption in a gas from saturated carbon. The solid line is a fit with a period of 160 cm^{-1}. (b) shows the fluorescence in this wavelength range. Data replotted from [21].

We have furthermore tested C_4F_{10} gas which had been partially cleaned only by molecular sieves 10 Å and activated carbon. The results are plotted in figure 8 (b). The solid line is a fit with C_2H_2 at 75 ppm, C_2H_4 at 0.025 ppm, other alkenes is set to 0 ppm and C_6H_6 at 0.05 ppm. The uncertainty on these parameters is estimated to be about 10 %. Oxygen and water are included with their measured value of 2 ppm. Rayleigh scattering is also added for the 5 meter scattering length.

The differences between the fit parameters in figure 8 (a) and (b) are striking. The amount of benzene has gone down by a factor of 6 between sample [a] and [b] and is thereby nearly absent in sample [b], acetylene is reduced by a factor of 2 and the class of alkenes have more or less disappeared. This is very reasonable considering that aromatic hydrocarbons like benzene are efficiently adsorbed by the carbon. Inspecting figure 6 we observe that acetylene and ethylene has a diameter below 4 Å and most of the other alkenes have a diameter between 4 and 5 Å. C_4F_{10} has a diameter of 5.6 Å. It will rapidly saturate the 10 Å sieve and the adsorption of these hydrocarbons will be very ineffective. It is furthermore not unlikely that some alkenes have been formed in sample [a] by the use of catalyst.

We have concluded from these results it is most probable that the loss of transparency is due to an admixture of hydrocarbons with double bonds. The most efficient way to clean the C_4F_{10} fluid should then be to apply molecular sieves 5 Å and activated carbon on the fluid. A large scale test of some 500 kg of raw C_4F_{10} fluid has been done and the result is shown in figure 10. An excellent fit to the data is obtained by adding 35 ppm of n-C_4H_{10} to the fit parameters which includes the Rayleigh scattering and the measured water and oxygen content in gas sample.

Clearly the amount of hydrocarbons which is acceptable in the fluids is a function of the absorption length of the detector system and of the cut-off wavelength of the photon detector. In the current test we have stopped the cleaning process since the effect of the admixture of n-C_4H_{10} is masked by the light transmission property of the quartz window on the photon detectors. Material losses by using molecular sieves of size $\leq$5Å will in general be small. CF_4 might pose a problem as it has a kinetic diameter of 4.7 Å. Activated carbon should be used to trap the highly absorbing aromatics as long as they influence the transparency of the fluid.

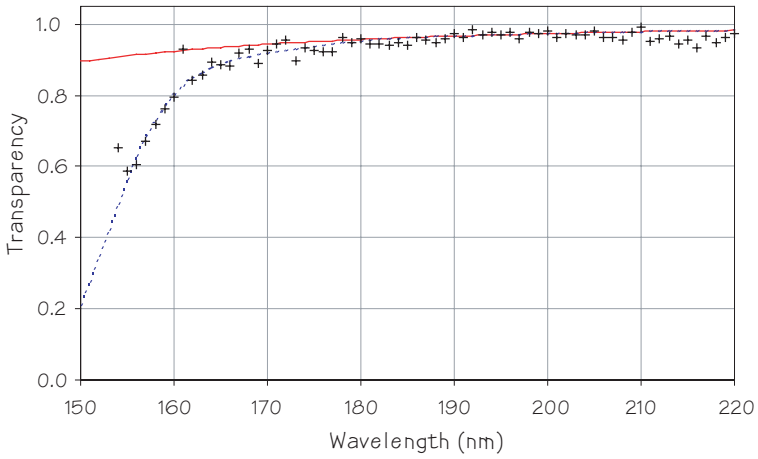

Figure 10: Transparency of C_4F_{10} for an absorption length of 186 cm at NTP. The solid line is Rayleigh scattering only. The dotted line shows the effect of adding 35 ppm of n-C_4H_{10} and the water and oxygen content which was measured to be 1 ppm.

7 Conclusion

We have argued that the loss of optical transparency in perfluorocarbons in the VUV range is due to an admixture of hydrocarbons. This admixture is most probably due to the production method of the fluorocarbons. Molecular sieves of 5 Å are very effective in removing most of these pollutants with only insignificant losses of raw material. Aromatic hydrocarbons like C_6H_6 can be isolated effectively with activated carbon. This will inevitably lead to a loss of fluorocarbons. In order to reduce the losses to a minimum, it is therefore preferable to monitor the need to use activated carbon.

We have furthermore shown that the use of dispersed Cu or Cr can greatly endanger the optical transparency of fluorocarbons if not fully fluorinated fluorocarbons are present in the fluid.

Acknowledgement

We are greatly indebted to many people at the different collaborating institutes who have with dedication contributed to the success of the various Cherenkov detector systems from which we have taken the data presented in this paper. We wish to express our gratitude and appreciation to all of them and in particular to V. Gracco, C. Joram and B. Nielsen at the DELPHI RICHs, F. Bradamante, G. Mallot and S. Paul at the COMPASS experiment and R. Gernhäuser of the HADES experiment at GSI for their patience and for their support of this work. We wish to express our greatest appreciation to A. Braem and M. Bosteels for their permanent technical support. We gratefully acknowledge the work of the Department of Chemistry, University of Milano, for the measurement of the mass spectra.

References

[1] P. Aarnio et al., The DELPHI Detector at LEP, Nucl. Instrum. Methods Phys. Res., A : 303(1991)233
M. Battaglia and P.M. Kluit, Particle identification using the DELPHI RICH detectors, Nucl. Instrum. Methods Phys. Res., A : 433(1999)252
K. Abe et al., Performance of the CRID at SLD, Nucl. Instrum. Methods Phys. Res., A : 343 (1994)74
R. J. Apsimon et al., A Ring Imaging Cherenkov detector for the CERN Omega Spectrometer – the design and recent performance, Nucl. Instrum. Methods Phys. Res., A : 248(1986)76

[2] R. Arnold et al., A RICH detector with a sodium fluoride radiator : π/K identification up to 3 GeV/c, Nucl. Instrum. Methods Phys. Res., A : 273 (1988)466
CLEO Collaboration, The CLEOIII ring imaging Cherenkov detector, Nucl. Instrum. Methods Phys. Res., A : 379(1996)448

[3] G. Baum et al., The COMPASS RICH project, Nucl. Instrum. Methods Phys. Res., A : 433 (1999)426
K. Zeitelhack et al., The HADES RICH Detector, Nucl. Instr. Meth. A : 433 (1999) 201
ALICE collaboration, Detector for High Momentum PID, CERN/LHCC 98-19, ALICE TDR 1, 14 August 1998

[4] R. Abjean et al., Refractive index of Carbon Tetrafluorid (CF_4) in the 300-140 nm wavelength range, Nucl. Instrum. Methods Phys. Res., A : 292(1990)593

[5] R. Abjean et al., Refractive index of hexafluoroethane (C_2F_6) in the 300-150 nm wavelength range, Nucl. Instrum. Methods Phys. Res., A : 354(1995)417
W.A. Gault and G.G. Shepherd, Dispersion and Refractivity of Gases for Interferometric Pressure-Scanning, Appl.Opt. 12(1973)1739

[6] A. Bideau-Mehu et al., Refractive index of octoflueropropane (C_3F_8) in the 300-150 nm wavelength range, Nucl. Instrum. Methods Phys. Res., A : 381(1996)576

[7] A. Filippas et al., Precision Measurements of Gas Refractivity by means of a Fabry-Perot Interferometer illustrated by the Monitoring of Radiator Refractivity in the DELPHI RICH Detectors, submitted to Elsevier Preprint, 2002.

[8] P.G. Moyssides et al., A VUV prism spectrometer for RICH radiator refractometry, J.Mod.Opt. : 47(2000)no.10, pp.1693

[9] C.D. Nenitescu, CHIMIE ORGANICA, Vol. 1, 1966

[10] E. Albrecht et al., The Radiator Gas and the Gas System of COMPASS RICH1, Preprint submitted to Elsevier Preprint 6 September 2002.

[11] J. Werner, K^s_0- und- Λ_0 Produktion und Nachweis von s-Baryonen mit dem zentralen ringabbildenden Cherenkovzaehler des DELPHI-Detektors auf der Z-Resonanz, Ph.D. thesis, University of Wuppertal. (Oct. 92).
G. Lenzen et al., The use of fluorocarbon radiators in the DELPHI RICH detectors, Nucl. Instrum. Methods Phys. Res., A : 343(1994)268
E. Schyns, Measurement of $\pi^{\pm}$, $K^{\pm}$, p and $\bar{p}$ production in $Z_0 \rightarrow q\bar{q}$, $Z_0 \rightarrow b\bar{b}$ and $Z_0 \rightarrow u\bar{u}$, $d\bar{d}$, $s\bar{s}$ (Particle Identification with the DELPHI Barrel Ring Imaging Cherenkov Counter), Ph.D. thesis, University of Wuppertal. (04/07/97)

[12] P. Baillon et al., An improved method for manufacturing accurate and cheap glass parabolic mirrors, Nucl. Instrum. Methods Phys. Res., A : 276(1988)492
P. Baillon et al., Production of 300 paraboloidal mirrors with high reflectivity for use in the Barrel RICH counter in DELPHI at LEP, Nucl. Instrum. Methods Phys. Res., A : 277(1988)338

[13] M.A. Gaspar, Current Monitor for the MSGC High Voltage Power Supply, Private communication, March 2001.

[14] 3M Product Manual, Fluorinert^{TM} Electronic Liquid, 1981

[15] K. Watanabe et al., Absorption Coefficients of Several Atmospheric Gases, AFCRC Technical Report No. 53-23, 1953

[16] M. Agawa, Absorption Cross Section of O_2 and CO_2 Continua in the Schumann and the Far-uv Region, J.Chem.Phys. 54, 4, 1971

[17] G.P. Anderson et al., Polynomial Coefficient for Calculating O_2 Schumann-Runge Cross Sections at 0.5 cm^{-1} Resolution, J.Geophys.Res. 97(1992)10,103

[18] J.G. Calvert and J.N. Pitts, Jr., Photochemistry, John Wiley & Sons, Inc. 1966.

[19] Jones, L.C., Jr.; Taylor, L.W., Far ultraviolet absorption spectra of unsaturated and aromatic hydrocarbons, Anal. Chem., 1955, 27, 2

[20] J. Romand et B. Vodar, Spectres d'absorption du benzène à l'ètat vapeur et l'ètat condensé dans l'utraviolet lointain, Comptes Rendus de l'Academie des Sciences (1951)233

[21] H. Sponer and G. Nordheim, Analysis of the Near Ultraviolet Electronic Transition of Benzene, J.Chem.Phys., 7,4(1939)207

[22] H. Du et al., PhotochemCAD: A computer-aided design and research tool in photochemistry, Photochemistry and Photobiology, 68, 141-142, 1998

[23] Y. Benilan et al., The long wavelength range temperature variations of the mid-UV acetylene absorption coefficient, Planetary and Space Science, 48(2000)463

[24] D.W. Breck, Zeolite Molecular Sieves, Structure, Chemestry, and Use, John Wiley & Sons 1974

[25] Y. Osada and T. Nakagawa (Editor), Membrane Science and Technology, Marcel Dekker 1992
Cadotte et al., Thin Film Composite Reverse-Osmosis Membranes: Origin, Development, and Recent Advances, in vol. I of Synthetic Membranes, ACS Symposium Series 153 (1981).

[26] S. Ilie and G. Lenzen, Perfluorocarbon Liquid. Specific Chemical Aspects for the use within the DELPHI RICH, DELPHI note 93-33 RICH 54.
H. Fürstenau et al., Separation of fluocarbons in the fluid systems of the DELPHI barrel RICH detector, Nucl. Instrum. Methods Phys. Res., A : 371(1996)263

[27] 3M Speciality Adhesives & Chemicals Analytical Laboratory / SMMD, Request # 59363, File Reference: k59363, October 6, 1999.